European Radiology (2019) 29:4529–4537
https://doi.org/10.1007/s00330-018-5969-y

CHEST

Feasibility of low-dose CT with spectral shaping and third-generation iterative reconstruction in evaluating interstitial lung diseases associated with connective tissue disease: an intra-individual comparison study

Xiaoli Xu[1] · Xin Sui[1] · Lan Song[1] · Yao Huang[1] · Yingqian Ge[2] · Zhengyu Jin[1] · Wei Song[1]

Received: 16 August 2018 / Revised: 30 October 2018 / Accepted: 13 December 2018 / Published online: 8 February 2019

Abstract

Objectives To investigate the feasibility of low-dose CT (LDCT) with tin filtration and third-generation iterative reconstruction (IR) in evaluating interstitial lung diseases associated with connective tissue disease (CTD-ILD).

Methods Fifty-three consecutive adult patients with CTD-ILD underwent regular-dose chest CT (RDCT) at 110 kVp followed by LDCT with tin-filtered 100 kVp. RDCT was reconstructed with filtered back projection (FBP) and advanced modeled iterative reconstruction (ADMIRE); LDCT was reconstructed with ADMIRE. Image noise, streak artifact, image quality, and visualization of normal and abnormal CT features were evaluated and compared among RDCT-ADMIRE, RDCT-FBP, and LDCT-ADMIRE groups.

Results The mean radiation dose of LDCT was reduced to 20% of RDCT. Objective image noise of RDCT-ADMIRE (38.08 ± 6.37 HU), LDCT-ADMIRE (51.68 ± 9.06 HU), and RDCT-FBP (62.09 ± 10.95 HU) increased progressively ($p < 0.001$ in any two pairs). RDCT-ADMIRE significantly improved subjective image noise, streak artifact, and overall image quality compared with RDCT-FBP and LDCT-ADMIRE (all $p < 0.001$), while no significant difference was noted between the latter two groups. All abnormal lung structures were better scored in RDCT-ADMIRE compared with those in RDCT-FBP (all $p < 0.001$). LDCT-ADMIRE was inferior to RDCT-FBP in visualizing peripheral bronchi and vessels as well as reticulation (all $p < 0.001$); other normal and abnormal structures were similar between the two groups.

Conclusion LDCT with tin filtration and third-generation IR was applicable in evaluating ILD lesions of CTD. Image quality was significantly improved after applying ADMIRE algorithm to CT protocols.

Key Points

- *Optimization of CT radiation dose is a clinical concern in patients with connective tissue disease.*
- *Spectral shaping and third-generation iterative reconstruction emerge as promising techniques in reducing radiation dose and acquiring desired image quality of CTD-ILD patients.*
- *The third-generation iterative reconstruction algorithm can optimize visualization of ILD patterns in low-dose CT.*

Keywords X-ray computed tomography · Connective tissue disease · Interstitial lung disease · Image reconstruction · Radiation dosage

✉ Xin Sui
suixin@pumch.cn

✉ Zhengyu Jin
jinzy@pumch.cn

✉ Wei Song
cjr.songwei@vip.163.com

[1] Department of Radiology, Peking Union Medical College Hospital, Chinese Academy of Medical Sciences, No.1 Shuaifuyuan Wangfujing Dongcheng District, Beijing 100730, China

[2] Siemens China, Beijing, China

Abbreviations

ADMIRE	Advanced modeled iterative reconstruction
AP	Anteroposterior
CT	Computed tomography
CTD	Connective tissue disease
CTD-ILD	Interstitial lung diseases associated with connective tissue disease
$CTDI_{vol}$	Volume CT dose index
DLP	Dose-length product

ED	Effective radiation dose
FBP	Filtered back projection
GGO	Ground-glass opacities
HRCT	High-resolution computed tomography
ILD	Interstitial lung disease
IR	Iterative reconstruction
LAT	Lateral
LDCT	Low-dose CT
RDCT	Regular-dose chest CT
SAFIRE	Sinogram-affirmed iterative reconstruction
SNR	Signal-to-noise ratio
SSDEs	Size-specific dose estimates

Introduction

Interstitial lung disease (ILD) is one of the most common and serious pulmonary complications of connective tissue diseases (CTD), serving as a substantial contributor to high mortality in CTD patients. The diagnosis of CTD-ILD is usually based on the synthesis of clinical, radiographic, laboratory, pulmonary function testing, and pathologic data [1]. Among which, high-resolution chest computed tomography (HRCT) is particularly indispensable for the detection, characterization, quantification, staging, prognosis, and treatment evaluation of ILD [2–4]. Even if lung involvement might be absent before therapy, HRCT is still inevitable during the treatment process because ILD can occur as a complication of treatment for CTD [5].

With the increasing application of CT, radiological communities have gradually recognized the potential harmful effects of excessive levels of ionizing radiation. Various strategies were thus proposed to reduce the applied radiation dose, including CT hardware and software optimization [6]. In recent years, automatic exposure control systems and iterative reconstruction (IR) algorithm were the mostly applied methods to decrease radiation dose while maintaining diagnostic image quality [7–9]. Some researchers found it promising in applying these dose-reduction techniques for CT assessment of ILD [10]. Pontana et al reported that chest CT images with sinogram-affirmed iterative reconstruction (SAFIRE) algorithm enabled 60% dose reduction of standard-dose CT without compromising evaluation of ILD [11]. Katsura et al announced that model-based iterative reconstruction (MBIR) could significantly improve the image quality of ILD compared with filtered back projection (FBP) [12].

Furthermore, a CT device with built-in tin filter for single-energy imaging was lately introduced. This technique is also known as spectral filtration or spectral shaping, when combined with the latest generation IR, advanced modeled iterative reconstruction (ADMIRE), a drastic dose reduction can be achieved in chest CT [13, 14]. Haubenreisser et al [15] compared tin-filtered 100 kVp with standard 100-kVp chest CT in a matched patient group and found that the former with ADMIRE rendered 90% radiation dose reduction and similar image quality compared with the latter with SAFIRE. Furthermore, several studies have verified the feasibility of low-dose chest CT (LDCT) with these new techniques in clinical settings, including evaluation of pulmonary nodules, infection as well as emphysema quantification, and lung volumetry, with radiation dose equivalent to chest radiography [16, 17]. However, no studies have assessed the detailed visualization of normal and abnormal lung structures of ILD in spectral shaping chest CT. Besides, the clinical utility of ADMIRE in evaluating CTD-ILD was not investigated so far.

CTD is characterized by various kinds of ILD patterns on CT images, and LDCT is considered promising for CTD-ILD evaluation and longitudinal monitoring, especially in those young and undergoing repetitive CT examinations. Therefore, CTD patients are considered an interesting population to explore the potential application of new dose-reduction techniques in assessing ILD lesions. The purpose of this study was to investigate the feasibility of low-dose CT with tin filtration and third-generation IR in evaluating CTD-ILD.

Materials and methods

Patients

This study was based on retrospective interpretation of prospectively acquired data over a 6-month period, which was approved by the institutional review board of our institution. Between January 2016 and June 2016, 53 consecutive adult patients (37 women, 16 men; mean age, 56.4 ± 11.1 years; range, 28–76 years) indicated for the diagnosis or follow-up of CTD-ILD were enrolled in this study. The population consisted of 14 Sjögren's syndrome, 11 rheumatoid arthritis, 10 mixed connective tissue disease, 7 polymyositis/dermatomyositis, 5 systemic sclerosis, 4 anti-neutrophil cytoplasmic antibody–associated vasculitis, and 2 systemic lupus erythematosus. The mean BMI was 24.3 ± 3.8 kg/m^2 (range, 17.3–35.6 kg/m^2). The procedure, involving acquisition of regular-dose chest CT (RDCT) followed by an additional low-dose CT (LDCT), was explained to the participants. Informed consent was obtained from each patient.

CT protocols

All CT scans were performed on a third-generation dual-source CT unit (SOMATOM Force; Siemens Healthcare). Each patient underwent two consecutive unenhanced CT scans in single-energy acquisition mode with supine position. First, RDCT was performed at 110 kVp tube voltage, 80 mAs reference tube current, 0.5 s gantry rotation time, and pitch 1.2. Afterwards, LDCT was operated with tin-filtered 100 kVp (Sn100 kVp), 250 mAs, 0.25 s, and pitch 2.0. Both RDCT and

LDCT were obtained at detector collimation of 192 × 0.6 mm with z-flying focal spot and applied with four-dimensional dose modulation system. RDCT scans were performed with automated attenuation-based tube potential selection (setting 3), and LDCT scans were at a fixed tube potential. The scan range was from the costophrenic angle to the pulmonary apex, including the entire lung parenchyma. Patients were asked to hold their breath at full inspiration during the examination.

Image reconstruction

RDCT images were reconstructed with both FBP and ADMIRE, and LDCT images were reconstructed with ADMIRE. ADMIRE was set at strength level of 3 [13]. All images were reconstructed with a slice thickness of 1 mm and increment of 0.5 mm in the axial plane using a corresponding lung kernel of Bl57. Images were then transmitted to a diagnostic workstation (Centricity RA1000; GE Yokogawa Medical Systems) for further data analysis.

Objective assessment of image quality

The objective assessment of noise was performed by drawing circular regions of interest within the tracheal lumen above the aortic arch (mean ± standard deviation of the region of interest surface 1.14 ± 0.38 cm^2; range 0.58–2.10 cm^2), which were placed by one radiologist with 6 years of experience in chest CT. Three measurements were performed and averaged for each region. The mean HU and its standard deviation were recorded. Image noise was defined as standard deviation of the attenuation value. The signal-to-noise ratio (SNR) was calculated as the ratio of attenuation value to noise.

Subjective assessment of image quality

Images were presented in a randomized order, and radiologists were all blinded to patients' image reconstruction techniques. Subjective image quality assessment was performed by three radiologists (with 6, 10, and 20 years of experience in thoracic CT, respectively) in consensus on the workstation. Image analysis was performed at preselected lung window settings (window level, − 400 HU; window width, 1500 HU); radiologists were allowed to moderately change the default window settings for ease of assessment.

(1) Evaluation of subjective image noise, streak artifacts, and overall image quality

Subjective image noise and streak artifacts were evaluated by a 3-point scale: 1 = unapparent or minimal, 2 = moderate but not alter the identification of normal and/or abnormal structures, 3 = severe and alter the identification of normal and/or abnormal structures [11]. Overall image quality was rated by using a 5-point scale: 1 = excellent; 2 = very good; 3 = satisfactory, with acceptable image quality; 4 = suboptimal, with limited diagnostic value; and 5 = non-diagnostic, with unacceptable image quality.

(2) Assessment of normal and abnormal lung structures

The normal structures evaluated were fissures, proximal bronchi and adjacent pulmonary vessels (above the subsegmental level), peripheral bronchi and adjacent pulmonary vessels (subsegmental and beyond the subsegmental level), and subpleural vessels (within 10 mm of the pleura) [11]. Five abnormal structures were examined at the lobar level, including six lobes per patient (the right upper, middle, and lower lobes; left upper culmen, lingula, and lower lobes) [11]. A total of 316 pulmonary lobes from 53 patients were included in the subjective analysis of abnormal lung structures; other two lobes presenting as lung atelectasis were excluded from the evaluation. The five abnormal structures analyzed were ground-glass opacities (GGO), reticulation, bronchiectasis and/or bronchiolectasis, architectural distortion, and honeycombing [18]. The visibility of normal and abnormal lung structures was rated on a 5-point scale: 1 = excellent image quality with sharp demarcation of structures; 2 = slight blurring of the structures, with unrestricted image evaluation; 3 = moderate blurring of the structures, with slight restricted assessment; 4 = severe blurring and poorly defined structures, with uncertainty about the evaluation; and 5 = severely reduced image quality, making reliable interpretation impossible. The rating of abnormal structures also included a score of 0 denoting the absence of abnormal signs [19].

Radiation dose estimation

For each CT acquisition, the volume CT dose index ($CTDI_{vol}$) and dose-length product (DLP) recorded on patient protocols were noted. The effective radiation dose (ED) was calculated by multiplying the DLP by a chest-specific conversion coefficient (0.014 mSv/mGy cm) [20]. Anteroposterior (AP) and lateral (LAT) dimensions at the mid-liver level were measured from axial CT images by using digital calipers. Based on the effective diameter of the chest $\left(\text{effective diameter} = \sqrt{\text{AP}\cdot\text{LAT}}\right)$, size-specific dose estimates (SSDEs) were calculated using the size-specific conversion factor f_{size} from AAPM Report204 ($SSDE = f_{size} \cdot CTDI_{vol}$) [21, 22].

Statistical analysis

Categorical variables were reported as frequencies or percentages and continuous variables as means ± standard deviation. The significance of differences of radiation dose between

RDCT and LDCT was tested using paired samples *t* tests or the Wilcoxon signed-rank test depending on the results of the Shapiro-Wilk test. Statistical differences of objective noise and subjective image quality scores among RDCT-ADMIRE, RDCT-FBP, and LDCT-ADMIRE groups were analyzed with the Friedman test followed by post hoc Dunn's test as a control. All statistical analyses were performed by using SPSS (SPSS 20.0, IBM). A two-tailed *p* value of less than 0.05 was considered to indicate statistical significance.

Results

Objective assessment of image quality

The mean CT value and image noise increased and SNR decreased progressively in RDCT-ADMIRE, LDCT-ADMIRE, and RDCT-FBP groups; statistical difference was significant between any two groups (all $p < 0.001$) (Table 1).

Subjective assessment of image quality

Subjective image quality scoring is displayed in Table 2. RDCT-ADMIRE significantly improved image noise as well as streak artifacts compared with RDCT-FBP and LDCT-ADMIRE (all $p < 0.001$), but no significant difference was noted between the latter two groups (*p* ranging from 0.361 to > 0.99). As to overall image quality, 100% of RDCT-ADMIRE images, 94.3% (50/53) of RDCT-FBP, and 84.9% (45/53) of LDCT-ADMIRE were acceptable (scores 1–3). Significant differences of overall image quality were shown in comparing RDCT-ADMIRE with RDCT-FBP and LDCT-ADMIRE (all $p < 0.001$), but no statistical difference was evident between the latter two groups ($p = 0.098$). No series of images were categorized as non-diagnostic (score, 5) in any group.

Image quality scoring of normal lung structures is summarized in Table 3. Fissure scoring of RDCT-ADMIRE was superior to that of RDCT-FBP and LDCT-ADMIRE (all $p < 0.001$), while no significant difference was observed between the latter two groups ($p > 0.99$). Proximal bronchus and vessel scoring of RDCT-ADMIRE was superior to that of LDCT-ADMIRE ($p = 0.031$), comparisons between other two groups showed no significant difference (all $p > 0.10$). Peripheral bronchus and vessel scoring of RDCT-ADMIRE and RDCT-FBP was remarkably superior to that of LDCT-ADMIRE (all $p < 0.001$); no significant difference was indicated between the former two groups ($p = 0.175$). Visibility of subpleural vessels of RDCT-ADMIRE was better than that of LDCT-ADMIRE ($p = 0.009$); comparisons between other two groups indicated no statistical difference (all $p > 0.30$).

Image quality scoring of abnormal lung structures is summarized in Table 4. GGO scores of RDCT-ADMIRE were significantly better than those of RDCT-FBP ($p < 0.001$); comparisons between the other two groups showed no significant difference (all $p > 0.05$). RDCT-ADMIRE was better in visualizing reticulation than RDCT-FBP and LDCT-ADMIRE (all $p < 0.001$); RDCT-FBP was also superior to LDCT-ADMIRE ($p < 0.001$) (Fig. 1). Bronchiectasis and bronchiolectasis scoring of RDCT-ADMIRE was better than that of RDCT-FBP and LDCT-ADMIRE (all $p < 0.001$); the latter two groups showed no statistical difference ($p = 0.440$). Architectural distortion and honeycombing scoring of RDCT-ADMIRE was remarkably superior to that of RDCT-FBP and LDCT-ADMIRE (all $p < 0.001$); no significant difference was indicated between the latter two groups ($p > 0.99$) (Fig. 2).

Radiation dose estimation

The radiation dose parameters are summarized in Table 5. $CTDI_{vol}$, DLP, ED, and SSDE in LDCT group were approximately reduced to 20% of RDCT group.

Discussion

This study sought to explore the feasibility of LDCT with spectral shaping and ADMIRE algorithm in evaluating CTD-ILD. The results demonstrated that LDCT with mean

Table 1 Objective assessment of image quality

Parameter	RDCT-FBP	RDCT-ADMIRE	LDCT-ADMIRE	*p* value[#]
CT value (HU)	− 949.81 ± 13.20	− 977.41 ± 9.12	− 962.88 ± 11.25	< 0.001
Noise (HU)	62.09 ± 10.95	38.08 ± 6.37	51.68 ± 9.06	< 0.001
SNR	15.76 ± 2.79	26.38 ± 4.47	19.18 ± 3.37	< 0.001

Data are mean ± SD

RDCT, regular-dose CT; *LDCT*, low-dose CT; *ADMIRE*, advanced modeled iterative reconstruction; *FBP*, filtered back projection

[#] *p* value in an overall comparison among RDCT-FBP, RDCT-ADMIRE, and LDCT-ADMIRE groups ($p < 0.001$ in any two groups)

Table 2 Evaluation of subjective image quality in three groups

Parameter	RDCT-FBP	RDCT-ADMIRE	LDCT-ADMIRE	*p* value[#]
Subjective noise (score)				< 0.001
Minimal (1)	4 (7.6)	50 (94.3)	3 (5.7)	
Moderate (2)	43 (81.1)	3 (5.7)	39 (73.6)	
Severe (3)	6 (11.3)	0	11 (20.7)	
Streak artifact (score)				< 0.001
Minimal (1)	12 (22.6)	44 (83.0)	2 (3.8)	
Moderate (2)	38 (71.7)	9 (17.0)	47 (88.7)	
Severe (3)	3 (5.7)	0	4 (7.5)	
Overall image quality (score)				< 0.001
Excellent (1)	0	4 (7.6)	0	
Very good (2)	16 (30.2)	44 (83.0)	3 (5.7)	
Satisfactory (3)	34 (64.1)	5 (9.4)	42 (79.2)	
Suboptimal (4)	3 (5.7)	0	8 (15.1)	
Non-diagnostic (5)	0	0	0	

Numbers are frequencies of images (total number of patients, 53) with percentages in parentheses

[#] *p* value in an overall comparison among RDCT-FBP, RDCT-ADMIRE, and LDCT-ADMIRE groups

ED of 0.35 mSv was applicable in assessing normal and abnormal structures of CTD-ILD when the new techniques were utilized. And the image quality was significantly improved after applying ADMIRE algorithm to CT protocols.

Table 3 Evaluation of normal lung structure visibility in three groups

Parameter	RDCT-FBP	RDCT-ADMIRE	LDCT-ADMIRE	*p* value[#]
Fissures (score)				< 0.001
Sharp delineation (1)	9 (17.0)	44 (83.0)	2 (3.8)	
Slight blurring (2)	43 (81.1)	9 (17.0)	51 (96.2)	
Moderate blurring (3)	1 (1.9)	0	0	
Severe blurring (4)	0	0	0	
Unreliable analysis (5)	0	0	0	
Proximal bronchi and vessels (score)				0.018
Sharp delineation (1)	51 (96.2)	53 (100)	47 (88.7)	
Slight blurring (2)	2 (3.8)	0	6 (11.3)	
Moderate blurring (3)	0	0	0	
Severe blurring (4)	0	0	0	
Unreliable analysis (5)	0	0	0	
Peripheral bronchi and vessels (score)				< 0.001
Sharp delineation (1)	40 (75.5)	53 (100)	14 (26.4)	
Slight blurring (2)	13 (24.5)	0	39 (73.6)	
Moderate blurring (3)	0	0	0	
Severe blurring (4)	0	0	0	
Unreliable analysis (5)	0	0	0	
Subpleural vessels (score)				< 0.001
Sharp delineation (1)	0	8 (15.1)	0	
Slight blurring (2)	48 (90.6)	45 (84.9)	39 (73.6)	
Moderate blurring (3)	5 (9.4)	0	13 (24.5)	
Severe blurring (4)	0	0	1 (1.9)	
Unreliable analysis (5)	0	0	0	

Numbers are frequencies of images (total number of patients, 53), with percentages in parentheses

[#] *p* value in an overall comparison among RDCT-FBP, RDCT-ADMIRE, and LDCT-ADMIRE groups

Table 4 Evaluation of abnormal lung structure visibility in three groups

Parameter	RDCT-FBP	RDCT-ADMIRE	LDCT-ADMIRE	*p* value[#]
Ground-glass opacity (score)				< 0.001
Absent (0)	4 (1.3)	4 (1.3)	4 (1.3)	
Sharp delineation (1)	0	38 (12)	0	
Slight blurring (2)	270 (85.4)	274 (86.7)	306 (96.8)	
Moderate blurring (3)	41 (13)	0	6 (1.9)	
Severe blurring (4)	1 (0.3)	0	0	
Unreliable analysis (5)	0	0	0	
Reticulation (score)				< 0.001
Absent (0)	8 (2.6)	8 (2.6)	8 (2.6)	
Sharp delineation (1)	2 (0.6)	75 (23.7)	0	
Slight blurring (2)	242 (76.6)	232 (73.4)	192 (60.8)	
Moderate blurring (3)	61 (19.3)	1 (0.3)	100 (31.6)	
Severe blurring (4)	3 (0.9)	0	16 (5.0)	
Unreliable analysis (5)	0	0	0	
Bronchiectasis and bronchiolectasis (score)				< 0.001
Absent (0)	87 (27.5)	87 (27.5)	87 (27.5)	
Sharp delineation (1)	0	82 (26)	3 (1)	
Slight blurring (2)	169 (53.5)	147 (46.5)	188 (59.5)	
Moderate blurring (3)	56 (17.7)	0	37 (11.7)	
Severe blurring (4)	4 (1.3)	0	1 (0.3)	
Unreliable analysis (5)	0	0	0	
Architectural distortion (score)				< 0.001
Absent (0)	14 (4.4)	14 (4.4)	14 (4.4)	
Sharp delineation (1)	6 (1.9)	97 (30.7)	2 (0.6)	
Slight blurring (2)	241 (76.3)	205 (64.9)	240 (76)	
Moderate blurring (3)	55 (17.4)	0	58 (18.4)	
Severe blurring (4)	0	0	2 (0.6)	
Unreliable analysis (5)	0	0	0	
Honeycombing (score)				< 0.001
Absent (0)	125 (39.6)	125 (39.6)	125 (39.6)	
Sharp delineation (1)	2 (0.6)	82 (26)	3 (0.9)	
Slight blurring (2)	138 (43.7)	109 (34.5)	140 (44.3)	
Moderate blurring (3)	47 (14.9)	0	43 (13.6)	
Severe blurring (4)	4 (1.2)	0	5 (1.6)	
Unreliable analysis (5)	0	0	0	

Numbers are frequencies of images (total number of lobes, 316), with percentages in parentheses

[#] *p* value in an overall comparison among RDCT-FBP, RDCT-ADMIRE, and LDCT-ADMIRE groups

Conventional FBP algorithm allows quick image reconstruction, but the reduction of radiation dose leads to noisy images with artifacts, which significantly compromises diagnostic confidence [23]. IR algorithms are now increasingly applied to reduce noise and artifacts from LDCT scans [24]. Several studies have reported the superiority of second-generation IR in assessing ILD over the first-generation IR or FBP [11, 12]. Katsura et al [12] verified that MBIR improved the image quality of ILD by reducing image noise and artifacts as well as elevating spatial resolution. However, MBIR requires image reconstruction time of 30–50 min, which would apparently limit its application in clinical practice.

The third-generation reconstruction algorithm, as applied in this study, combines an iterative approach statistical data modeling in the raw data domain with model-based noise detection in the image domain; it incorporates not only nearest-neighbor data but also a larger neighborhood on an anatomically reasonable length scale compared with SAFIRE. Therefore, ADMIRE renders higher image quality

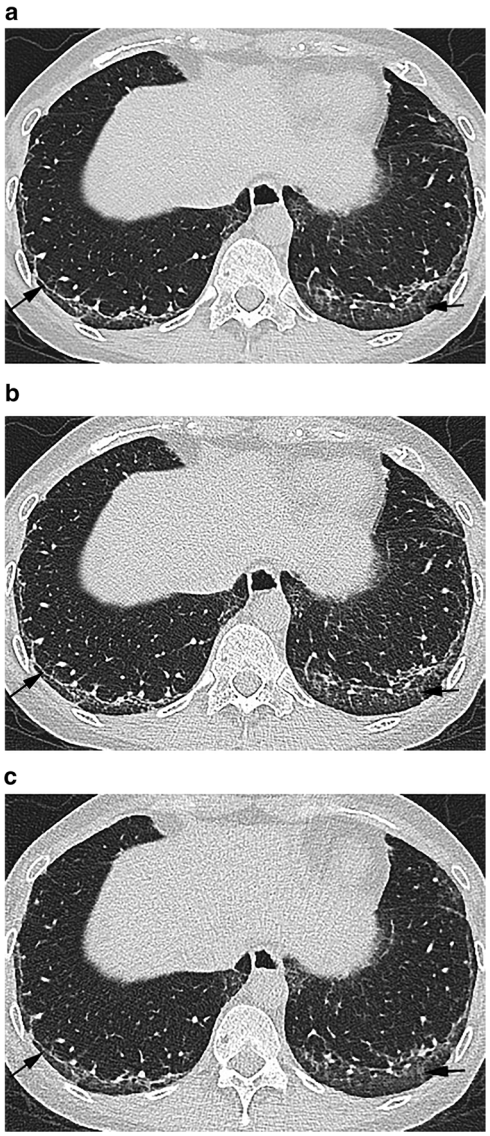

Fig. 1 High-resolution CT of a 31-year-old woman (BMI 18.4 kg/m^2) diagnosed as interstitial lung disease associated with polymyositis. CT features in (**a**) regular-dose image reconstructed with ADMIRE were all better depicted than that in (**b**) regular-dose image reconstructed with FBP and (**c**) low-dose image reconstructed with ADMIRE, including ground-glass opacity, reticulation, bronchiectasis, and architectural distortion in both lower lobes. Reticulation (black arrows) in **c** was less visualized compared with that in **a** and **b**. Objective noise was 31.48 HU on **a** images, 38.47 HU on **c** images, and 50.2 HU on **b** images

and more radiation dose reduction than SAFIRE [13]. Besides, the reconstruction time of ADMIRE requires only less than 1 min per setting, which would be more pragmatic in clinical use compared with MBIR, especially in emergency setting [24]. In this study, we compared ADMIRE and FBP in the RDCT protocol and found that overall image quality of RDCT-ADMIRE was remarkably superior to that of RDCT-FBP. Lung fissure and abnormal lung structure scoring of RDCT-ADMIRE all preceded that of RDCT-FBP, displaying the obvious advantage of ADMIRE algorithm in improving

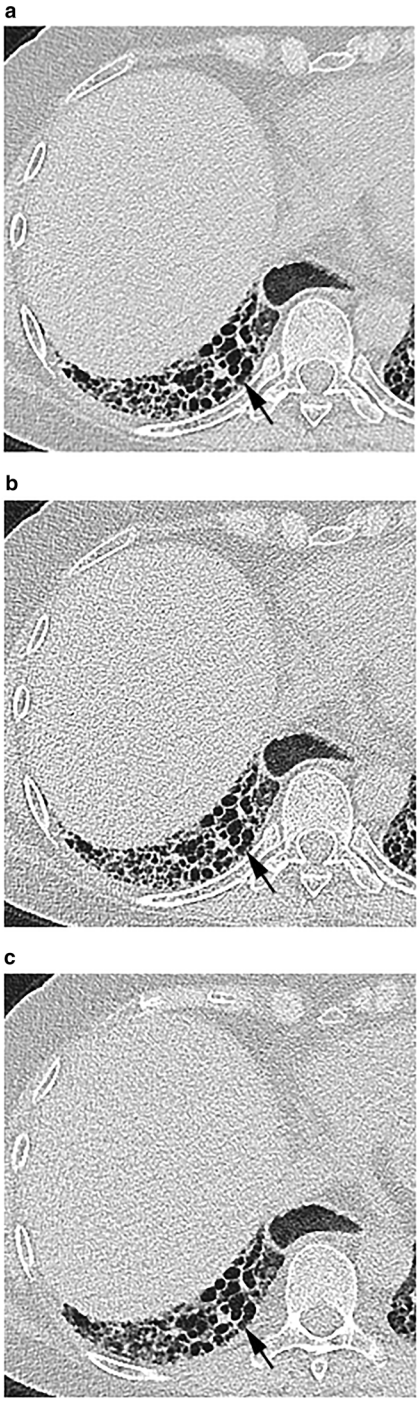

Fig. 2 High-resolution CT of a 55-year-old woman (BMI 22.3 kg/m^2) diagnosed as interstitial lung disease associated with Sjögren's syndrome. CT features in (**a**) regular-dose image reconstructed with ADMIRE were all better visualized than that in (**b**) regular-dose image reconstructed with FBP and (**c**) low-dose image reconstructed with ADMIRE, including ground-glass opacity, reticulation, bronchiectasis, architectural distortion, and honeycombing in the right lower lobe. Visibility of honeycombing (black arrows) was similar between **b** and **c**. Objective noise was 33.09 HU on **a** images, 49.78 HU on **c** images, and 53.33 HU on **b** images

Table 5 Radiation dose of regular-dose CT and low-dose CT

	RDCT	LDCT	*p* value
$CTDI_{vol}$ (mGy)	3.84 ± 0.88 (2.46–6.1)	0.81 ± 0.14 (0.52–1.14)	< 0.001
DLP (mGy·cm)	127.58 ± 34.90 (54.4–221.1)	25.14 ± 4.96 (16.5–38.4)	< 0.001
ED (mSv)	1.79 ± 0.49 (0.76–3.10)	0.35 ± 0.70 (0.23–0.54)	< 0.001
SSDEs (mGy)	5.24 ± 0.87 (3.82–7.70)	1.10 ± 0.12 (0.77–1.34)	< 0.001

Data are mean ± SD (range)

$CTDI_{vol}$, volume CT dose index; *DLP*, dose-length product; *ED*, effective radiation dose; *SSDEs*, size-specific dose estimates

image quality and visualization of ILD lesions. However, other normal lung structures showed no significant difference between the two groups; it is probably due to the apparent contrast effect of low attenuation of lung tissue that allows bronchi and pulmonary vessels less affected in the noisy FBP images [13].

Furthermore, the tin filter could remove the less dose-efficient low-energy photons from the X-ray spectrum and elevates the mean photon energy of the applied radiation so as to reduce the overall radiation dose; when combined with ADMIRE, even more dose efficiency can be achieved [15]. However, the extent of dose reduction is actually dependent on the acceptability of acquired image quality in the task. Detailed assessment of ILD usually requires higher image quality compared with evaluation of lung nodule or infection. Braun et al [25] reported that spectral filtration protocol with average ED of 0.24 mSv showed less diagnostic confidence compared with regular-dose group in evaluating ILD, while good diagnostic confidence was achieved in assessing pleural pathologies, pulmonary nodules, or pneumonia. Martini et al [16] found that, with average ED of 0.1 mSv, the sensitivity of tin filtration and ADMIRE protocol in detecting interstitial lung changes was 78–88%, and specificity was 96%. In the present study, we elevated the reference tube current in the applied tin-filtered 100-kVp protocol so as to improve the image quality of CTD-ILD, with mean ED of 0.35 mSv in LDCT group. It revealed that LDCT-ADMIRE presented no inferiority to RDCT-FBP in evaluating overall image quality. Except for peripheral bronchi and vessels as well as reticulation, subjective scores of normal and abnormal lung structures were all comparable between LDCT-ADMIRE and RDCT-FBP groups.

Although image noise and streak artifact in LDCT-ADMIRE were rated non-inferior to RDCT-FBP group, spatial resolution of images could be affected as the radiation dose significantly reduced. In this study, LDCT-ADMIRE was inferior in assessment of peripheral bronchi and vessels as well as reticulation to RDCT-FBP. Both groups were 100% diagnostically acceptable in evaluating peripheral bronchi and vessels. However, only 79.7% of RDCT FBP and 63.3% of LDCT ADMIRE images were diagnostically acceptable in evaluation of reticulation. Although IR enables improvement of SNR and spatial resolution, noise and spatial resolution are affected in a non-linear manner, which allows substantial noise reduction while maintaining spatial resolution of high-contrast objects and degrading spatial resolution of low-contrast objects in LDCT [11, 26]. Honeycombing is such a high-contrast feature, which explains the similar ratings between RDCT-FBP and LDCT-ADMIRE groups in our study. However, reticulation and GGO are low-contrast features that can be easily affected by obvious decrease of both SNR and spatial resolution in LDCT [26]. In this study, the inferiority in assessing reticulation could be attributed to the degradation of spatial resolution in low-dose scanning. However, GGO scoring showed no evident difference between LDCT-ADMIRE and RDCT-FBP groups. This was consistent with previous studies, which confirmed that IR of LDCT enabled non-inferior low-contrast spatial resolution in detecting and characterizing GGO compared with full-dose FBP images [26, 27].

This study was limited in several aspects. First, the study population was small due to the low prevalence of CTD and limited availability of desired patients. Second, inter-observer agreement for subjective image quality was not evaluated considering the substantial variability in assessing ILD [28, 29]; we preferred evaluating all factors in a consensus way. Third, the degree of inspiration may differ between LDCT and RDCT in the same patient because LDCT was performed after RDCT within a short time interval. Last, the LDCT ADMIRE group was inferior in evaluating reticulation, but we did not explore the optimal radiation dose in visualizing reticulation; further studies may be needed.

In conclusion, low-dose non-enhanced chest CT performed at tin-filtered 100 kVp with ADMIRE is feasible in evaluating CTD-ILD with average ED of 0.35 mSv, except for its limitation in assessing reticulation. ADMIRE markedly improves the image quality and visualization of lung structures, which can be proposed to evaluate patients with CTD-ILD in clinical routine instead of FBP, and further extended to the entire spectrum of ILDs.

Funding This study was supported by the National Public Welfare Basic Scientific Research Project (2017PT32004).

Compliance with ethical standards

Guarantor The scientific guarantor of this publication is Zhengyu Jin.

Conflict of interest Yingqian Ge is an employee of Siemens. She had no control on the study raw data and analysis.

Statistics and biometry No complex statistical methods were necessary for this paper.

Informed consent Written informed consent was obtained from all patients in this study.

Ethical approval Institutional Review Board approval of Peking Union Medical College Hospital was obtained.

Methodology
- retrospective
- observational study
- performed at one institution

Publisher's note Springer Nature remains neutral with regard to jurisdictional claims in published maps and institutional affiliations.

References

1. Vij R, Strek ME (2013) Diagnosis and treatment of connective tissue disease-associated interstitial lung disease. Chest 143:814–824
2. Walsh SL, Sverzellati N, Devaraj A, Keir GJ, Wells AU, Hansell DM (2014) Connective tissue disease related fibrotic lung disease: high resolution computed tomographic and pulmonary function indices as prognostic determinants. Thorax 69:216–222
3. Fischer A, Lee JS, Cottin V (2015) Interstitial lung disease evaluation: detecting connective tissue disease. Respiration 90:177–184
4. Goh NS, Desai SR, Veeraraghavan S et al (2008) Interstitial lung disease in systemic sclerosis: a simple staging system. Am J Respir Crit Care Med 177:1248–1254
5. Mathai SC, Danoff SK (2016) Management of interstitial lung disease associated with connective tissue disease. BMJ 352:h6819
6. Bankier AA, Tack D (2010) Dose reduction strategies for thoracic multidetector computed tomography: background, current issues, and recommendations. J Thorac Imaging 25:278–288
7. Baumueller S, Winklehner A, Karlo C et al (2012) Low-dose CT of the lung: potential value of iterative reconstructions. Eur Radiol 22:2597–2606
8. Lee SW, Kim Y, Shim SS et al (2014) Image quality assessment of ultra low-dose chest CT using sinogram-affirmed iterative reconstruction. Eur Radiol 24:817–826
9. McCollough CH, Bruesewitz MR, Kofler JM Jr (2006) CT dose reduction and dose management tools: overview of available options. Radiographics 26:503–512
10. Ohno Y, Koyama H, Yoshikawa T, Seki S (2015) State-of-the-art imaging of the lung for connective tissue disease (CTD). Curr Rheumatol Rep 17:69
11. Pontana F, Billard AS, Duhamel A et al (2016) Effect of iterative reconstruction on the detection of systemic sclerosis-related interstitial lung disease: clinical experience in 55 patients. Radiology 279:297–305
12. Katsura M, Sato J, Akahane M, Mise Y, Sumida K, Abe O (2017) Effects of pure and hybrid iterative reconstruction algorithms on high-resolution computed tomography in the evaluation of interstitial lung disease. Eur J Radiol 93:243–251
13. Gordic S, Morsbach F, Schmidt B et al (2014) Ultralow-dose chest computed tomography for pulmonary nodule detection: first performance evaluation of single energy scanning with spectral shaping. Invest Radiol 49:465–473
14. Newell JD Jr, Fuld MK, Allmendinger T et al (2015) Very low-dose (0.15 mGy) chest CT protocols using the COPDGene 2 test object and a third-generation dual-source CT scanner with corresponding third-generation iterative reconstruction software. Invest Radiol 50:40–45
15. Haubenreisser H, Meyer M, Sudarski S, Allmendinger T, Schoenberg SO, Henzler T (2015) Unenhanced third-generation dual-source chest CT using a tin filter for spectral shaping at 100kVp. Eur J Radiol 84:1608–1613
16. Martini K, Barth BK, Nguyen-Kim TD, Baumueller S, Alkadhi H, Frauenfelder T (2016) Evaluation of pulmonary nodules and infection on chest CT with radiation dose equivalent to chest radiography: prospective intra-individual comparison study to standard dose CT. Eur J Radiol 85:360–365
17. Messerli M, Ottilinger T, Warschkow R et al (2017) Emphysema quantification and lung volumetry in chest X-ray equivalent ultra-low dose CT - intra-individual comparison with standard dose CT. Eur J Radiol 91:1–9
18. Hansell DM, Bankier AA, MacMahon H, McLoud TC, Müller NL, Remy J (2008) Fleischner Society: glossary of terms for thoracic imaging. Radiology 246:697–722
19. Studler U, Gluecker T, Bongartz G, Roth J, Steinbrich W (2005) Image quality from high-resolution CT of the lung: comparison of axial scans and of sections reconstructed from volumetric data acquired using MDCT. AJR Am J Roentgenol 185:602–607
20. The measurement, reporting, and management of radiation dose in CT: AAPM report no. 96. 2008. (Accessed 23 Feb 2015, at www.aapm.org/pubs/reports/rpt_96.pdf)
21. Christner JA, Braun NN, Jacobsen MC, Carter RE, Kofler JM, McCollough CH (2012) Size-specific dose estimates for adult patients at CT of the torso. Radiology 265:841–847
22. AAPM Task Group 204 (2011) Size-specific dose estimates (SSDE) in pediatric and adult body CT examinations. Report of AAPM Task Group 204
23. Pan X, Sidky EY, Vannier M (2009) Why do commercial CT scanners still employ traditional, filtered back-projection for image reconstruction? Inverse Probl 25:1230009
24. Khawaja RD, Singh S, Otrakji A et al (2015) Dose reduction in pediatric abdominal CT: use of iterative reconstruction techniques across different CT platforms. Pediatr Radiol 45:1046–1055
25. Braun FM, Johnson TR, Sommer WH, Thierfelder KM, Meinel FG (2015) Chest CT using spectral filtration: radiation dose, image quality, and spectrum of clinical utility. Eur Radiol 25:1598–1606
26. McCollough CH, Yu L, Kofler JM et al (2015) Degradation of CT low-contrast spatial resolution due to the use of iterative reconstruction and reduced dose levels. Radiology 276:499–506
27. Christe A, Charimo-Torrente J, Roychoudhury K, Vock P, Roos JE (2013) Accuracy of low-dose computed tomography (CT) for detecting and characterizing the most common CT-patterns of pulmonary disease. Eur J Radiol 82:e142–e150
28. Walsh SL, Calandriello L, Sverzellati N, Wells AU, Hansell DM (2016) Interobserver agreement for the ATS/ERS/JRS/ALAT criteria for a UIP pattern on CT. Thorax 71:45–51
29. Watadani T, Sakai F, Johkoh T et al (2013) Interobserver variability in the CT assessment of honeycombing in the lungs. Radiology 266:936–944